A new path in defining light parameters for hair growth: discovery and modulation of photoreceptors in human hair follicle

Serena Buscone, BSc [1,2], Andrei N Mardaryev MD, PhD [1], Bianca Raafs, BSc [2], Jan W Bikker [3], Carsten Sticht, PhD [4], Norbert Gretz MD, PhD [4], Nilofer Farjo, MD [5], Natallia E. Uzunbajakava, PhD[2*], Natalia V Botchkareva MD, PhD [1*]

[1] Centre for Skin Sciences, Faculty of Life Sciences, University of Bradford, Bradford, West Yorkshire, United Kingdom, BD7 1DP; [2] Philips Research, High Tech Campus 34, Eindhoven, The Netherlands, 5656 AE; [3] Consultants in Quantitative Methods BV, Eindhoven, The Netherlands; [4] Center of Medical Research, Faculty Mannheim, University of Heidelberg, Germany; [5] Farjo Hair Institute, Manchester, UK

Author contributions: S.B. performed experiments and data analysis, wrote the manuscript; B.R. gave technical support; J.W.B. performed statistical analysis on the hair follicle response to light *ex vivo*; C.S. and N.G. conducted microarray and bioinformatics analysis; N.F. contributed to tissue sample collection; N.E.U, A.N.M. and N.V.B. jointly conceived and supervised the study, and edited the manuscript.

Financial Disclosure: This study was supported by the European Marie-Curie Actions Programme, Grant agreement no.: 607886 to S. Buscone (Early Stage Researcher), N.E. Uzunbajakava and A.N. Mardaryev (scientific supervisors), N.V. Botchkareva (scientific supervisor, principal investigator).

Conflict of Interest Disclosures: Natallia E. Uzunbajakava, and Bianca Raafs are the employee of Philips Electronics Netherland B.V. and received salary for this study.

***Corresponding authors:**
Dr. Natalia V. Botchkareva, MD, Centre for Skin Sciences. University of Bradford, Richmond Road, Bradford, West Yorkshire BD7 1DP, England, Tel: +44 (0) 1274 233 795, E-mail: n.botchkareva@bradford.ac.uk

Dr. ir. Natallia E. Uzunbajakava, Philips Research, High Tech Campus 34, 5656 AE, Eindhoven, The Netherlands, Tel: +31 6 397 68 141, E-mail: natallia.uzunbajakava@philips.com

Key words: Hair follicle, hair cycle, hair follicle stem cells, outer root sheath, photobiomodulation, blue light, Opsin 2, Opsin 3

Abstract

Background and Objective: Though devices for hair growth based on low levels of light have shown encouraging results, further improvements of their efficacy is impeded by a lack of knowledge on the exact molecular targets that mediate physiological response in skin and hair follicle. The aim of this study was to investigate the expression of selected light-sensitive receptors in the human hair follicle and to study the impact of UV-free blue light on hair growth *ex vivo*.

Material and Methods: The expression of Opsin receptors in human skin and hair follicles has been characterised using RT-qPCR and immunofluorescence approaches. The functional significance of Opsin 3 was assessed by silencing its expression in the hair follicle cells followed by a transcriptomic profiling. Proprietary LED-based devices emitting two discrete visible wavelengths were used to access the effects of selected optical parameters on hair growth *ex vivo* and outer root sheath cells *in vitro*.

Results: The expression of OPN2 (Rhodopsin) and OPN3 (Panopsin, Encephalopsin) was detected in the distinct compartments of skin and anagen hair follicle. Treatment with 3.2 J/cm^2 of blue light with 453 nm central wavelength significantly prolonged anagen phase in hair follicles *ex vivo* that was correlated with sustained proliferation in the light-treated samples. In contrast, hair follicle treatment with 3.2 J/cm^2 of 689 nm light (red light) did not significantly affect hair growth ex vivo. Silencing of OPN3 in the hair follicle outer root sheath cells resulted in the altered expression of genes involved in the control of proliferation and apoptosis, and abrogated stimulatory effects of blue light (3.2 J/cm^2; 453 nm) on proliferation in the outer root sheath cells.

Conclusions: We provide the first evidence that 1) OPN2 and OPN3 are expressed in human hair follicle, and 2) 453 nm blue light at low radiant exposure exerts a positive effect on hair growth ex vivo, potentially via interaction with OPN3.

Introduction

Photobiomodulation (PBM) has been clinically reported to have a positive impact on hair growth (1-3), skin rejuvenation (4,5), wound healing (6-8), psoriasis (9,10) and eczema (11). The lack of the risk of potential systemic side effects is well recognized as benefits in treatment of cutaneous disorders (12,13). Up to now the list of light-based devices for the management of hair regrowth with FDA 510k premarket notification clearance counts thirty two entries (1-3). The efficacy of light-based therapy is reported to be similar to that of existing FDA-approved drugs (minoxidil and finasteride) (13). However, a recent review highlighted the significant differences in the choice of optical parameters used by available devices that are still claimed to have clinically comparable hair growth-stimulating efficacy (14).

From our perspective, the inconsistency in the choice of optical parameters can be addressed by filling the current gap in fact-based knowledge of the key molecular receptors that mediate the effects of light: in the field of PBM experimental-based evidence on how photons are received by cells is vaguely present, while the recent review discussed about at least 10 classes of photosensor proteins and additional photosensitive domains involved in molecular mechanisms used by biological systems to detect light (15).

The pioneering work of Dr Tiina Karu suggested that cytochrome *c* oxidase plays a role of a light acceptor with absorption bands in red and near-infrared (NIR) range (650 – 980 nm) and even higher (about ten times) extinction coefficient in a blue-green spectral range (around 400-500 nm) (16). It was shown that irradiation of cytochrome *c* oxidase using blue, red and near-infrared light was able to modulate not only metabolic activity, but also gene expression(17); however, the majority of PBM-based devices are solely relying on red and NIR- spectral components.

In recent years, several molecules have emerged as novel mediators of light activation in non-photosensitive tissues, such as nitrosated proteins regulating nitric oxide (NO) (18-21) and the flavoprotein-containing cryptochromes that are also involved in the regulation of the circadian rhythm (22). They are all absorbing in the blue part of the electromagnetic spectrum. Increasing evidence suggest that an additional class of light-sensitive receptors, Opsins, is expressed in a varieties of tissues outside the vision mediating retina (23,24). Opsins can be divided into two sub-families: 1) visual Opsins, including Opsin 1 (short, middle and long wavelength) present in cone cells and mediate colour vision, and Opsin 2 (Rhodopsin), a dim-light vision mediator that is expressed in rod cells; 2) non-visual Opsins, including Opsin 3 (Panopsin or Encephalopsin), Opsin 4 (Melanopsin) and Opsin 5 (Neuropsin) (25). All these receptors are characterized by specific absorption spectra and could act as G-protein-coupled receptors (GPCRs) mediating different signal transduction cascades (26). In functional Opsins, a retinal molecule binds to a highly conserved lysine residue (27). In the presence of light, *cis* retinal is isomerized to all-*trans* retinal, and the straightening of the polyene chain activates the opsin (28).

Recent studies have revealed that the distinct members of the Opsin family are present in human skin and could contribute to skin homeostasis (23). For example, OPN2 expression was found in both human epidermal keratinocytes and melanocytes (29). A single exposure to violet light (380 – 410 nm) activated OPN2 and supressed keratinocyte differentiation (30). In human melanocytes, OPN2 was found to contribute to photo-transduction of ultraviolet A radiation (UVA) to increase melanin synthesis (29). OPN3 expression was found in retina, as well as in the cells outside of visual system, which suggest that OPN3 might function as a photoreceptor in various tissues (31,32). Interestingly, a homolog of the vertebrate OPN3 maintained photosensitive properties *in vitro* after transfection in mammalian cells, suggesting

that OPN3 homologs might have same ability to bind the non-conventional isomer 13-cis retinal to form an active photopigment (33,34).

It must be noted that the exact position of the absorption band in both OPN2 and OPN3 depends on the amino-acid sequence on the type of cis retinal bound (7- 9-cis, 11-cis, 13-cis) (35), and also on dark versus light conditions (28). Interestingly, the respective spectral sensitivity of rhodopsin through animal kingdom may cover an extremely broad range of the sunlight spectrum from 358 nm (near ultraviolet, UVA) to 630 nm (red) (36). OPN3 was shown to be a bi-stable pigment absorbing in the region of 400-530 nm, generating a stable photoproduct and reverting to its original state upon subsequent light absorption rather than undergoing photobleaching (33).

The aim of this study was to investigate the expression of selected light-sensitive receptors in the human hair follicle and to study the impact of blue light on hair growth *ex vivo*.

Materials and Methods

Human skin and hair follicle collection and culture

Human skin was obtained from either the temporal or occipital scalp regions of female and male donors, and from the beard region of male donors undergoing elective cosmetic surgery (total n=12, age 32-70). Tissue was obtained with full written consent adhering to the Declaration of Helsinki principles, following ethical and institutional approval under human tissue act guidelines.

RNA extraction and RT-PCR analysis

Microdissected HFs were collected in 1 ml of TRIzol® (Life technologies), mechanically homogenized and stored at -80°C. RNA isolation was performed using Direct-zol™ RNA MiniPrep kit (Zymo research). cDNA was synthesised by reverse transcription using the

High-Capacity cDNA Reverse Transcription Kit (Applied Biosystems™). PCR reactions were performed with primers corresponding to the retinal-binding site of human Opsins 1, 3, 4 and 5 (**Table 1**) touchdown PCR protocol as previously published (24). For amplification of OPN2 (**Table 1**) standard PCR conditions were employed: 95°C for 2 min, followed by 34 cycles of denaturation (95°C for 20 s), annealing (51°C for 20 s), and elongation (72°C for 30 s).

Quantitative RT-PCR was performed with SYBR Green Supermix (Applied Biosystems), using 10 ng cDNA and 1 μM primers (**Table 2**), and StepOnePlus^{TM} real-time PCR system (Applied Biosystems). Differences between samples were calculated using the Genex^{TM} software (Bio-Rad) based on the Ct ($C_t^{\Delta\Delta}$) equitation method and normalized to the housekeeping GAPDH gene. Total RNA from the human eye (Amsbio) and from HaCaT cell lines was used as the positive control.

Immunofluorescence

Six-μm cryosections were briefly air-dried followed by fixation in acetone (10 min, 20°C) or in 4% PFA (10 min, room temperature). The cryosections were incubated with 5% BSA for 1 hour at room temperature (Sigma) followed by application of optimal dilutions of primary antibodies over-night at 4°C (**Table 3**). Subsequently, sections were incubated with corresponding secondary antibodies, Alexa 488 or Alexa 647 (Invitrogen) for 1 hour at 37°C. Incubation steps were interspersed by four washes with phosphate buffer-saline (PBS 1x, 5 min each). Cell nuclei were counterstained using VECTASHIELD® mounting medium containing DAPI (Vector Labs). Image analysis was performed using a fluorescent microscope in combination with DS-C1 digital camera and ACT-2U image analysis software (Nikon).

Hair follicle stem cell sorting

Hair follicle stem cells were obtained from the scalp skin of 3 female donors (44-, 66 - and 70-years-old) as published before (37). Briefly, microdissected skin was incubated with Dispase I (Roche) overnight at 4°C followed by the separation of epidermis and the HFs from the dermis using forceps. At least 50 HFs were treated with 0.05% trypsin- 0.02% EDTA at 37°C for 30 min. Enzymatic digestion was neutralized by 10% FBS in PBS. Cells were filtered through a 40 um nylon mesh filter, pelleted by centrifuging at 170 g for 5 minutes and re-suspended in PBS with 0.5% BSA. Cells were stained with a mix of anti-human PE-conjugated CD200 (eBioscience), APC-CD34 (eBioscience) and FITC-CD49f integrin (eBioscience) antibodies for 30 min at 4°C followed by 15 minutes incubation with 7-AAD (BD Pharmingen) on ice to identify living cells. Two stem cell populations, CD200+/CD49f+ and CD34+/CD49f+, were sorted using Moflo XDP cell sorter (Beckman Coulter), and collected in TRIzol® LS Reagent (Life technologies) for total RNA isolation.

Cell culture and transfection

Primary human outer root sheath (ORS) keratinocytes were isolated from anagen HFs as described previously (37) and cultured in Keratinocyte Growth Medium 2 supplemented with Bovine Pituitary Extract 0.004 ml / ml, Epidermal Growth Factor (recombinant human) 0.125 ng/ml, Insulin (recombinant human) 5 μg/ml, Hydrocortisone 0.33 μg/ml, Epinephrine 0.39 μg/ml, Transferrin-holo (human) 10 μg/ml, and $CaCl_2$ 0.06 mM (Promocell) for no more than 3 passages. For OPN3 knockdown, ORS cells were transfected with 50 nM of smartpool siRNAs directed against OPN3 (ON-Targetplus) and a non-targeting control (Dharmacon) using Lipofectamine (RNAiMax, Invitrogen) according to the manufacturers' protocol.

Microarray and bioinformatic analysis

Total RNA was extracted from the ORS cells 48 hours post OPN3 siRNA transfection as described above. RNA was tested by capillary electrophoresis on an Agilent 2100 bioanalyzer

(Agilent) and high quality was confirmed. Gene expression profiling was performed using arrays of human HTA-2_0-st-type from Affymetrix. Biotinylated antisense cRNA was then prepared according to the Affymetrix standard labelling protocol with the GeneChip® WT Plus Reagent Kit and the GeneChip® Hybridization, Wash and Stain Kit (both from Affymetrix, Santa Clara, USA). Afterwards, the hybridization on the chip was performed on a GeneChip Hybridization oven 640, then dyed in the GeneChip Fluidics Station 450 and thereafter scanned with a GeneChip Scanner 3000. All of the equipment used was from the Affymetrix-Company (Affymetrix, High Wycombe, UK). A Custom CDF Version 20 with ENTREZ based gene definitions was used to annotate the arrays (38). The Raw fluorescence intensity values were normalized applying quantile normalization and RMA background correction. ANOVA was performed to identify differential expressed genes using a commercial software package SAS JMP10 Genomics, version 6, from SAS (SAS Institute, Cary, NC, USA). A false positive rate of a=0.05 with FDR correction was taken as the level of significance.

Light treatment

Microdissected HFs from 7 donors (53-55 year old) were cultured in phenol red-free Williams E medium (Life Technology) supplemented with hydrocortisone 10 ng/ml (Sigma-Aldrich), L-glutamine 2 mM (Sigma-Aldrich), and Penicillin 1000 U/ml / Streptomycin 1mg/ml, with or without 10 µg/ml insulin (Sigma-Aldrich) (39). Williams E medium contains traces of retinol. Since HF cells are known to possess a system for synthesis and metabolism of retinoids (62), no cis-retinal was added to the culture medium. HFs were cultured at 37°C in a humidified atmosphere of 5% CO_2 up to 14 days. Light treatment was performed using two proprietary LED-based devices with flat homogeneous illumination over the area of 24-well plates. Each device was emitting one discrete wavelength: 453 nm central wavelength, 16 nm full width half maximum (PHILIPS, The Netherlands) previously used for the

experiments on *in vitro* human cells study and in human clinical trials (18,40), and 689 nm central wavelength, 24 nm full width half maximum (PHILIPS, The Netherlands). Separate groups of HFs were treated daily using 453 nm or 689 nm wavelengths, 16mW/cm^2 irradiance, 3.2 J/cm^2 radiant exposures during 10 consecutive days. Optical power was measured before each experiment using Nova II power meter (Ophir Optronics Solutions Ltd) at the plane of HFs, assuring delivery of the correct irradiance (watts per area). No increase in temperature above 37°C was observed as monitored using FLIR A655sc Infrared Camera, (FLIR® Systems, Inc). Culture medium was refreshed every other day over the period of light treatment following the protocol of Mignon et al (41). The images were taken with wide-field microscope (Leica) for morphological evaluation.

Alamar Blue® metabolic activity assay

Primary ORS keratinocytes were seeded into 24 well-plate with a black frame (Porvair) at a density of 60000 cells per well, and cultured in fully supplemented phenol red free Keratinocyte Growth Medium 2 (Promocell). The cell mono-layers were treated with 3.2 J/cm^2 light (453 nm) using a proprietary LED-based device as described above. The changes in metabolic activity were assessed 24 hours after irradiation, using the Alamar Blue® assay (Thermofisher) following the manufacturer protocol. The fluorescence intensity of the supernatant was measured using a temperature controlled plate reader (FLUOstar OPTIMA, BMG Labtech).

EdU incorporation assay

ORS cells were grown on coverslips coated with 0.5% gelatin and treated with 3.2 J/cm^2 light (453 nm) as described above (n=4). To investigate if OPN3 is involved in mediating the effects of blue light cells were transfected with either scrambled siRNA (control) or siRNA against OPN3 after their exposure to 3.2 J/cm2 light (453 nm) as described above. After the

light treatment cells were incubated with fresh media containing 10 uM of the thymidine analogue EdU that incorporates into newly synthesized DNA (Click-iT® EdU Imaging Kits, Invitrogen). The cells were fixed in 4% PFA (10 minutes, room temperature). EdU detection was assessed following the manufacturer protocol. Cell nuclei were counterstained using VECTASHIELD® mounting medium containing DAPI (Vector Labs). Image acquisition was performed using a fluorescent microscope in combination with DS-C1 digital camera and ACT-2U image analysis software (Nikon). The percentage of proliferating cells was calculated from the total number of cells. Image J software was employed for image analysis.

Statistical analysis

For the analysis of HF growth *ex vivo*, the effects of medium, donor, and light treatments on mean survival time with standard errors, were based on a random-effects interval-data regression model. A commercial software package was used: StataCorp. 2015. Stata Statistical Software: Release 14. College Station, TX: StataCorp LP. T-test and Two-way ANOVA was performed using GraphPad Prism version 6.04 for Windows, GraphPad Software, La Jolla California USA, www.graphpad.com.

Results

Light-sensitive receptors, Opsin 2 and Opsin 3 are expressed in the human hair follicle

To investigate the expression of putative molecular targets for light therapy in human anagen HFs, a screening of Opsin receptor transcripts was performed by RT-PCR. Primers encompassing the Lysin residue that is required for the photo-activation of Opsin receptors were employed for OPN1SW, OPN1MW, OPN2 (Rhodopsin), OPN3 (Panopsin or Encephalopsin), OPN4 (Melanopsin), and OPN5 (Neuropsin) (24). RNA isolated from human

retina was used as a positive control. Only specific PCR products corresponding to OPN2 and OPN3 were detected in the HFs, whilst the expression of other Opsins was not observed (**Figure 1A**). To compare the relative levels of Opsins in anagen HF, RT-qPCR analysis was performed that revealed the higher OPN2 expression compared to OPN3 in 5 out of 6 samples analysed; such expression pattern was sex and age independent (**Figure 1B**).

Immuno-fluorescence analysis was performed to characterize the localization of detected light-sensitive receptors in skin. Prominent expression of OPN2 was seen in the epidermis and in dermal fibroblasts in skin obtained from either male beard or female scalp regions (**Figure 2A, B,** respectively). OPN2 expression was co-localized with cytokeratin 14 (CK14), suggesting the presence of OPN2 in the basal epidermal layer (**Figure 2B**). In the HF, the expression of OPN2 was restricted to the lower and upper ORS (**Figure 2C**). Similar pattern of OPN2 expression was detected in terminal (**Figure 2D**) and vellus HFs (**Figure 2E**). In addition, OPN2 expression was seen in the HF compartment harbouring the stem cells (bulge) as demonstrated by the double staining of OPN2 with a stem cell marker CD200 (**Figure 2F-G)**.

Analysis of OPN3 expression revealed its presence in the epidermal layers, as well as in the dermis (**Figure 3A**). In the HFs, OPN3 expression was predominantly seen in the inner root sheath (IRS). Similar pattern of OPN3 expression was seen in the terminal HFs derived from the scalp (**Figure 3B**) and vellus HFs (**Figure 3C**). IRS specific OPN3 expression was further confirmed by double-immunolabelling with AE15 that detects trichohyalin, an intermediate filament-associated protein involved in the IRS differentiation (**Figure 3D**). Expression of OPN3 was not detected in the hair cortex as it was confirmed by a double-immunostaining with a marker AE13 (**Figure 3E**).

In addition, the expression of OPN2 and OPN3 was investigated in the follicular stem cells (HFSC) isolated from anagen HFs, using a combination of antibodies against CD200, CD34

and CD49f-integrin markers, as described previously (42) (**Figure 4A**). CD200 is a cell-surface marker of the epithelial HFSC found in the bulge region, while CD34 is expressed in the HFSC of the suprabulbar ORS (42-45). By qPCR, *OPN2* and *OPN3* transcripts were detected in both CD200+ and CD34+ cell populations from 3 female donors of different age (43, 66 and 70-y-o) (**Figure 4B**).

Because expression of OPN3 was detected in the keratinocytes of the IRS that do not undergo proliferation, the effect of OPN3 silencing was evaluated in highly proliferative cultured ORS cells. RT-PCR analysis confirmed expression of *OPN3* transcripts in these cells (**Figure 5A)**. Silencing of OPN3 did not cause any gross changes on cell morphology (**Figure 5 B)**. Efficiency of OPN3 silencing was confirmed by real-time PCR analysis: over 80% decline in *OPN3* transcript level was observed in siRNA - OPN3 treated cells comparing to the control (**Figure 5 C**). Microarray analysis of the global gene expression in the ORS keratinocytes treated with OPN3 siRNA or corresponding control revealed the altered expression of 41 genes (**Table 4**): 37 were downregulated, while only 4 were upregulated due to OPN3 knockdown. Microarray validation by qPCR confirmed that the expression of UL16 binding protein 1 (ULBP1), p21 protein (Cdc42/Rac)-activated kinase (PAK2), follistatin-like 1 (FSTL1) and ubiquitin protein ligase E3 component N-recognin 5 (UBR5) was downregulated in the ORS cells after OPN3 silencing (**Figure 5E**). In contrast, the expression of sideroflexin 1 (SFNX1), caveolin 2 (CAV2) and biogenesis of lysosomal organelles complex 1 subunit 2 (BLOC1S2) was increased due to OPN3 silencing in the ORS cells (**Figure 5E**).

Taken together, our data assert that light-sensitive receptors OPN2 and OPN3 are expressed in the epidermal and HF keratinocytes, including HFSC; their specific localization might suggest their implication in epidermal and HF homeostasis.

Blue light prolongs anagen hair growth phase *ex vivo*

Blue light could interact with a variety of photoactive proteins: NADPH oxidase, nitrozated proteins (18,20), light-activated enzyme, cytochrome c oxidase (46) , intracellular calcium and light-gated ion channels (47), and circadian photoreceptors cryptochromes 1 and 2 (48). This could further activate secondary messengers, like nitric oxide and other ROS, cAMP, ATP and Ca2+ (14). Such a versatile range of photochemical reactions has a potential to trigger photobiological effects underlying the therapeutic action of PBM (49).

As both Opsins 2 and 3 have also absorption bands in the blue-to-green region (33,34) we tested the impact of 453 nm wavelength light on hair growth by performing daily irradiation of HFs *ex vivo* during 10 consecutive days.

Recently we have demonstrated stimulatory effect of low radiant exposure, 2 J/cm^2 of blue 450 nm light on reticular and papillary dermal fibroblasts (41). Therefore, irradiance and radiant exposure were set to low levels (16 mW/cm^2 irradiance, 200 sec illumination duration, 3.2 J/cm^2 radiant exposure) to assure initiation of purely photobiological effects and to avoid any photothermal reactions.

We have also evaluated the impact of low levels of red light (689 nm, 16 mW/cm^2 and 3.2 J/cm^2). While this frequency most probably lies outside of the absorption band of discovered Opsins, we included it in our experiments as red wavelength at low radiant exposure is most often used in *in vitro* and animal experiments and in the devices for *in vivo* hair growth (1,3). It also falls within the absorption spectrum of cytochrome c oxidase, a chromophore that is often attributed to be responsible for PBM-mediated effects (50-52).

HFs were divided into different groups: a control group was kept in the dark, while treated groups were exposed daily to either red or blue light during 10 days. Culture medium was refreshed every other day after light irradiation. HF gross morphology was monitored daily

using a wide-field microscope to distinguish anagen and catagen phases (**Figure 6A**). An interval regression with random intercept model was applied to analyse anagen to catagen transition, where mean survival time of a HF in culture (anagen maintenance) was selected as a measure. Effects of medium, donor and light treatments on mean survival time from 7 independent experiments are shown in **Figure 6 B**. HF growth in the media without insulin was used as a positive control for this study. Insulin depletion caused significant premature catagen development (p=0) that is consistent with previously published data (53). A donor effect was also statistically significant (p=0.012). This has confirmed the applicability and quality of the statistical model. A radiant exposure of 3.2 J/cm^2 of blue light has increased mean survival time of HF *ex vivo*, improving anagen maintenance (pairwise comparison control versus blue light significant at 10% level, p=0.066) (**Figure 6 B).** In contrast, HF treatment with 3.2 J/cm^2 of 689 nm light (red light) did not significantly affect hair growth compared to the untreated control (pairwise comparison control versus red light, p=0.7) (**Figure 6 B).** Positive effects of blue light on hair growth was further confirmed by the assessment of proliferation in HFs: the number of proliferative Ki-67+ cells was significantly increased at day 2 post treatment with low level of blue light compared to the control (p=0.04) (**Figure 6 C**).

In addition, low level of blue light (3.2 J/cm^2, 450 nm), stimulated metabolic activity of the ORS keratinocytes *in vitro*, as it was determined by the Alamar assay (p=0.05) (**Figure 6 D**) and significantly (p=0.004) increased proliferation compared to the control cells (**Figure 6 E**). Interestingly, silencing of OPN3 abrogated stimulatory effects of blue light (3.2 J/cm^2, 453 nm) on proliferation in the ORS cells (**Figure 6 F**). Significant inhibition (p<0.0001) in proliferation rate was observed in the ORS cells treated with blue light and transfected with OPN3 siRNA compared to the cells treated with blue light and transfected with control (scrambled) siRNA (**Figure 6 F**).

Discussion

Over the last decades, PBM has been suggested as an approach for hair loss treatment alternative to drugs. Several clinical studies reported encouraging results demonstrating the increase in hair density and thickness in response to red and near infrared light-based therapy (54). However, the exact molecular mechanism underlying light-mediated hair regrowth remain largely unknown (2,55).

The effect of PBM is triggered by the interaction of low levels of light with endogenous chromophores and photoreceptors in the skin (14,56). There is a rich spectrum of molecules absorbing optical radiation over the whole visible and near-infrared range (14,56).

The effects of blue light could be mediated by photolytic generation of NO from nitrozated proteins (18,20), ROS formation as a result of enzymatic reactions of e.g. NADPH oxidase (57), and cytochrome c oxydase (46). Alternatively, it could be mediated by photoactive pigments or chromophores (including the flavins and retinal) bound to cryptochromes 1 and 2 (48), intracellular calcium and light-gated ion channels (47), and opsin family proteins (29,30). Light interaction with all these potential molecular targets could lead to multiple downstream reactions, such as changes in pH, [Ca2+], cAMP, ATP, NO) (14,47).

Despite of such a long list of potential absorbers of blue light, the shorter-wavelength UV-free part of the electromagnetic spectrum remains to be relatively unexplored. The latter could possibly be explained by a relatively short penetration depth of this part of the electromagnetic spectrum. However, 450 nm light is successfully used for treatment of cutaneous diseases, including psoriasis and eczema (10,11), suggesting sufficient blue light penetration into the skin. Additional optical beam manipulations (58) might allow the photons of blue light at sufficient density to reach HF epithelial cells, including the bulge stem cells located in the outer root sheath.

In this study, we showed for the first time that OPN2 and OPN3, the photoreceptors absorbing light in visible blue-green wavelength range, are expressed in human skin, epithelial and mesenchymal components, and in the distinct compartments of the anagen HFs. Our data are in consistence with the study of Denda *et al* who demonstrated the expression of OPN2 in the human epidermal keratinocytes (23). In addition, we observed specific OPN2 expression in the basal layer keratinocytes expressing Keratin 14 (**Figure 2 B)**. Intriguingly, the expression of both OPN2 and OPN3 was detected in the HF stem cells (**Figure 4**).

These findings suggest that the activity of HF stem cells might be modulated by blue-green visible light within the absorption band of discovered Opsins directly interacting with them and activating GPCR-related pathways or via more complex reaction cascades, involving additional chromophores or photoreceptors, for example, cytochrome *c* oxidase, nitrosated proteins, cryptochromes, and others. Interestingly, transcriptomic analysis revealed that silencing of OPN3 expression in the proliferating ORS keratinocytes leads to the altered expression of genes involved in the control of stem cell activity in skin and hair follicle (**Figure 5**). For example, the expression of p21-activated kinase 2 (PAK2) and follistatin-like1 (FSTL1) was downregulated due to OPN3 silencing. PAK2 plays a role in a variety of different signaling pathways including cytoskeleton regulation, cell motility, apoptosis or proliferation. PAK2 acts as a downstream effector of RAC1 that leads to the inhibition of c-Myc (59,60). Both RAC1 and c-Myc are implicated in the control of epidermal stem cell (61). FSTL1 inhibits bone morphogenetic protein (BMP) suppressive effects in telogen HF stem cells allowing the initiation of the new hair cycle (62). Furthermore, *in vitro* analysis of the effect of OPN3 downregulation on cell proliferation revealed the significant decrease in the number of proliferative EdU positive cells compared to the corresponding controls (**Figure 6 F**), highlighting a novel previously unrecognised role for OPN3 in cell cycle modulation in the HF cells.

Photosensitivity of visual Opsins requires biding of the 11-cis-retinal chromophore to a Lysin residue of the G protein coupled receptors; while 11-cis retinal is abundantly present in the eye to ensure the formation of a functional receptor, all-trans retinals are mostly present in non-photosensitive tissues (33,63). Nevertheless, it has been reported that homologs of vertebrate OPN3 in pufferfish and mosquito becomes light sensitive when it is bound to 13-cis-retinal, and it might function as photoreceptors in many tissues (63). Therefore, the expression of OPN2 and OPN3 in the different HF compartments stimulated our interest in understanding the physiological role for Opsins in hair growth and their possible involvement in light sensing capability of the HF.

It has been demonstrated that keratinocyte irradiation with blue light of 412-426 nm at relatively high radiant exposure causes toxic effects (18). In addition, 41.4 J/cm^2 453 nm blue light irradiation rapidly induces ROS production and anti-proliferative effects (18,64).

In our study, we observed that low level of light at 453 nm wavelength (which falls within Opsins absorption spectrum) perpetuate anagen phase in HF *ex vivo* associated with sustained proliferation in the hair matrix keratinocytes that was diminished in the untreated control (**Figure 6**). Interestingly, low radiant exposure of 3.2 J/cm^2 stimulated metabolic activity in the ORS cells and promoted their proliferation (**Figure 6**). A positive effect of low levels of 453 nm blue light has recently been demonstrated in the dermal fibroblasts: the activation of metabolic activity and even more, the increased collagen production by papillary fibroblasts (41), and increased total protein synthesis (65). Therefore, these reports suggest that low levels of blue light could promote positive effects on cell growth and functions. In line with it, our study demonstrated that 3.2 J/cm^2 of blue light with 453 nm central wavelength exert beneficial effect on anagen maintenance of HF ex vivo. Interestingly, the stimulatory effect of blue light on proliferation was negated by silencing of OPN3: downregulation of OPN3 *in vitro* dramatically reduced proliferation rate, which was induced by blue light treatment in

primary ORS cells (**Figure 6**). These findings support our hypothesis that positive effects of blue light on hair growth could be mediated, at least in part, by light-sensitive receptors such as OPN3.

Despite numerous existing publications about responsiveness of HFs and HF cells to red light and existing commercial red light-emitting devices for hair growth stimulation, in our study 3.2 J/cm^2 of 689 nm light (red light) did not significantly affect hair growth *ex vivo* (p=0.7). However, this lack of statistical significance does not necessarily serve as evidence of the absence of positive effect of red light. We have recently published Viewpoint review (14) that summarizes the investigation of 90 reports published between 1985 and 2015, mostly based on application of red and near-infrared light. This investigation identified major inconsistencies in optical parameters between the published studies: a variety of the optical ranges of photon density applied in *in vitro* and *ex vivo* settings has been shown to extent over two orders of magnitude. Strikingly, same or very similar optical parameters used in different studies have been reported to trigger diverse effects on the cell (18,66-68); in addition, culture conditions can also have a huge impact on the outcome of the experiment (41). Therefore, we would like to emphasize the importance of careful experimental design in combination with well-characterized optical devices and biological models.

Conclusion

We provide the first evidence that OPN2 and OPN3 are expressed in human HF, and that 453 nm blue light at low radiant exposure exerts a positive effect on hair growth *ex vivo*, potentially via interaction with OPN3. The further research should be conducted to decipher interactions between blue light and Opsin receptors in the HFs, as well as to investigate a role of other blue-light acceptors in the control of hair growth. In addition, the beneficial effect of

blue light at low radiant exposure on hair growth raises a possibility of increasing therapeutic efficacy when combined with topical chemistry used for management of hair growth.

Acknowledgments. This study was supported by the European Marie-Curie Actions Programme, Grant agreement no.: 607886, to S. Buscone (Early Stage Researcher), N.E. Uzunbajakava (scientific supervisor), A.N. Mardaryev (scientific supervisor), N.V. Botchkareva (scientific supervisor, principal investigator).

List of Abbreviations

7-AAD, 7-aminoactinomycin D

AE 13, Hair cortex cytokeratin

AE 15, Trichohyalin

APC, Allophycocyanin

BLOC1S2, Biogenesis of lysosomal organelles complex 1 subunit 2

BMP, Bone morphogenetic protein

BSA, Bovine serum albumin

CAV2, Caveolin 2

CD200, OX-2 membrane glycoprotein

CD34, Hematopoietic progenitor cell antigen CD34

CD49f integrin, Integrin alpha 6

cDNA, Complementary deoxyribonucleic acid

CK 14, Cytokeratin 14

DAPI , 4',6-diamidino-2-phenylindole

EDTA, Ethylenediaminetetraacetic acid

EdU, 5-ethynyl-2′-deoxyuridine

FBS, Fetal bovine serum

FDA, Food and Drug Administration

FDR, False discovery rate

FITC, Fluorescein isothiocyanate

FSTL1, Follistatin-like 1

GAPDH, Glyceraldehyde 3-phosphate dehydrogenase

GPCR, G-protein-coupled receptors

HaCaT, Immortalized cultured human keratinocytes cell line

HF, Hair follicle

HFSC, Hair follicle stem cells

IRS, Inner root sheath

LED, Light-emitting diode

NIR, Near-infrared

NO, Nitric oxide

OPN1sw, Opsin 1 short wavelength

OPN1sw, Opsin 1 middle wavelength

OPN2, Opsin 2, Rhodopsin

OPN3, Opsin 3, Encephalopsin

OPN4, Opsin 4, Melanopsin

OPN5, Opsin 5, Neuropsin

ORS, Outer root sheath

PAK2, p21 protein (Cdc42/Rac)-activated kinase

PBM, Photobiomodulation

PBS, Phosphate-buffered saline

PCR, Polymerase chain reaction

PE, Phycoerythrin

PFA, Paraformaldehyde

qPCR, Quantitative polymerase chain reaction

RNA, Ribonucleic acid

ROS, Reactive oxygen species

RT-PCR, Reverse transcription polymerase chain reaction

RT-qPCR, Reverse transcription-quantitative Polymerase chain reaction

SFNX1, Sideroflexin 1

siRNA, Small interfering RNA

siSc, siRNA scrambled (negative RNA control)

siOPN3, siRNA against OPN3

UBR5, Ubiquitin protein ligase E3 component N-recognin 5

ULBP1, UL16 binding protein 1

UVA, Ultraviolet A

References

1. Lanzafame RJ, Blanche RR, Bodian AB, Chiacchierini RP, Fernandez-Obregon A, Kazmirek ER. The growth of human scalp hair mediated by visible red light laser and LED sources in males. Lasers in surgery and medicine 2013; 45(8):487-495.
2. Jimenez JJ, Wikramanayake TC, Bergfeld W, Hordinsky M, Hickman JG, Hamblin MR, Schachner LA. Efficacy and safety of a low-level laser device in the treatment of male and female pattern hair loss: a multicenter, randomized, sham device-controlled, double-blind study. Am J Clin Dermatol 2014; 15(2):115-127.
3. Lanzafame RJ, Blanche RR, Chiacchierini RP, Kazmirek ER, Sklar JA. The growth of human scalp hair in females using visible red light laser and LED sources. Lasers in surgery and medicine 2014; 46(8):601-607.
4. Dierickx CC, Anderson RR. Visible light treatment of photoaging. Dermatol Ther 2005; 18(3):191-208.
5. Rinaldi F. Laser: a review. Clin Dermatol 2008; 26(6):590-601.
6. Kajagar BM, Godhi AS, Pandit A, Khatri S. Efficacy of low level laser therapy on wound healing in patients with chronic diabetic foot ulcers-a randomised control trial. Indian J Surg 2012; 74(5):359-363.
7. Hopkins JT, McLoda TA, Seegmiller JG, David Baxter G. Low-Level Laser Therapy Facilitates Superficial Wound Healing in Humans: A Triple-Blind, Sham-Controlled Study. J Athl Train 2004; 39(3):223-229.
8. Gupta AK, Filonenko N, Salansky N, Sauder DN. The use of low energy photon therapy (LEPT) in venous leg ulcers: a double-blind, placebo-controlled study. Dermatol Surg 1998; 24(12):1383-1386.

9. Weinstabl A, Hoff-Lesch S, Merk HF, von Felbert V. Prospective randomized study on the efficacy of blue light in the treatment of psoriasis vulgaris. Dermatology 2011; 223(3):251-259.

10. Pfaff S, Liebmann J, Born M, Merk HF, von Felbert V. Prospective Randomized Long-Term Study on the Efficacy and Safety of UV-Free Blue Light for Treating Mild Psoriasis Vulgaris. Dermatology 2015; 231(1):24-34.

11. Keemss K, Pfaff SC, Born M, Liebmann J, Merk HF, von Felbert V. Prospective, Randomized Study on the Efficacy and Safety of Local UV-Free Blue Light Treatment of Eczema. Dermatology 2016; 232(4):496-502.

12. Metelitsa AI, Green JB. Home-use laser and light devices for the skin: an update. Semin Cutan Med Surg 2011; 30(3):144-147.

13. Mysore V. Finasteride and sexual side effects. Indian Dermatol Online J 2012; 3(1):62-65.

14. Mignon C, Botchkareva NV, Uzunbajakava NE, Tobin DJ. Photobiomodulation devices for hair regrowth and wound healing: a therapy full of promise but a literature full of confusion. Exp Dermatol 2016.

15. Porter ML. Beyond the Eye: Molecular Evolution of Extraocular Photoreception. Integr Comp Biol 2016.

16. Mason MG, Nicholls P, Cooper CE. Re-evaluation of the near infrared spectra of mitochondrial cytochrome c oxidase: Implications for non invasive in vivo monitoring of tissues. Biochim Biophys Acta 2014; 1837(11):1882-1891.

17. Karu T. Photobiology of low-power laser effects. Health physics 1989; 56(5):691-704.

18. Liebmann J, Born M, Kolb-Bachofen V. Blue-light irradiation regulates proliferation and differentiation in human skin cells. The Journal of investigative dermatology 2010; 130(1):259-269.

19. Keszler A, Brandal G, Baumgardt S, Ge ZD, Pratt PF, Riess ML, Bienengraeber M. Far red/near infrared light-induced protection against cardiac ischemia and reperfusion injury remains intact under diabetic conditions and is independent of nitric oxide synthase. Front Physiol 2014; 5:305.

20. Oplander C, Deck A, Volkmar CM, Kirsch M, Liebmann J, Born M, van Abeelen F, van Faassen EE, Kroncke KD, Windolf J, Suschek CV. Mechanism and biological relevance of blue-light (420-453 nm)-induced nonenzymatic nitric oxide generation from photolabile nitric oxide derivates in human skin in vitro and in vivo. Free Radic Biol Med 2013; 65:1363-1377.

21. Awakowicz P, Bibinov N, Born M, Busse B, Gesche R, Helmke A, Kaemling A, Kolb-Bachofen V, Kovacs R, Kuehn S, Liebmann J, Mertens N, Niemann U, Oplaender C, Porteanu HE, Scherer J, Suschek C, Vioel W, Wandke D. Biological Stimulation of the Human Skin Applying HealthPromoting Light and Plasma Sources. Contributions to Plasma Physics 2009; 49(9):641-647.

22. Bouly JP, Schleicher E, Dionisio-Sese M, Vandenbussche F, Van Der Straeten D, Bakrim N, Meier S, Batschauer A, Galland P, Bittl R, Ahmad M. Cryptochrome blue light photoreceptors are activated through interconversion of flavin redox states. The Journal of biological chemistry 2007; 282(13):9383-9391.

23. Tsutsumi M, Ikeyama K, Denda S, Nakanishi J, Fuziwara S, Aoki H, Denda M. Expressions of rod and cone photoreceptor-like proteins in human epidermis. Exp Dermatol 2009; 18(6):567-570.

24. Haltaufderhyde K, Ozdeslik RN, Wicks NL, Najera JA, Oancea E. Opsin expression in human epidermal skin. Photochemistry and photobiology 2015; 91(1):117-123.

25. Terakita A. The opsins. Genome Biol 2005; 6(3):213.

26. Porter ML, Blasic JR, Bok MJ, Cameron EG, Pringle T, Cronin TW, Robinson PR. Shedding new light on opsin evolution. Proc Biol Sci 2012; 279(1726):3-14.

27. Palczewski K. G protein-coupled receptor rhodopsin. Annual review of biochemistry 2006; 75:743-767.

28. Menon ST, Han M, Sakmar TP. Rhodopsin: structural basis of molecular physiology. Physiological reviews 2001; 81(4):1659-1688.

29. Wicks NL, Chan JW, Najera JA, Ciriello JM, Oancea E. UVA phototransduction drives early melanin synthesis in human melanocytes. Current biology : CB 2011; 21(22):1906-1911.

30. Kim HJ, Son ED, Jung JY, Choi H, Lee TR, Shin DW. Violet light down-regulates the expression of specific differentiation markers through Rhodopsin in normal human epidermal keratinocytes. PLoS One 2013; 8(9):e73678.

31. Halford S, Freedman MS, Bellingham J, Inglis SL, Poopalasundaram S, Soni BG, Foster RG, Hunt DM. Characterization of a novel human opsin gene with wide tissue expression and identification of embedded and flanking genes on chromosome 1q43. Genomics 2001; 72(2):203-208.

32. White JH, Chiano M, Wigglesworth M, Geske R, Riley J, White N, Hall S, Zhu G, Maurio F, Savage T, Anderson W, Cordy J, Ducceschi M, investigators G, Vestbo J, Pillai SG. Identification of a novel asthma susceptibility gene on chromosome 1qter and its functional evaluation. Hum Mol Genet 2008; 17(13):1890-1903.

33. Koyanagi M, Takada E, Nagata T, Tsukamoto H, Terakita A. Homologs of vertebrate Opn3 potentially serve as a light sensor in nonphotoreceptive tissue. Proceedings of the National Academy of Sciences of the United States of America 2013; 110(13):4998-5003.

34. Sugihara T, Nagata T, Mason B, Koyanagi M, Terakita A. Absorption Characteristics of Vertebrate Non-Visual Opsin, Opn3. PLoS One 2016; 11(8):e0161215.

35. Sekharan S, Morokuma K. Why 11-cis-retinal? Why not 7-cis-, 9-cis-, or 13-cis-retinal in the eye? J Am Chem Soc 2011; 133(47):19052-19055.

36. Luck M, Mathes T, Bruun S, Fudim R, Hagedorn R, Tran Nguyen TM, Kateriya S, Kennis JT, Hildebrandt P, Hegemann P. A photochromic histidine kinase rhodopsin (HKR1) that is bimodally switched by ultraviolet and blue light. The Journal of biological chemistry 2012; 287(47):40083-40090.

37. Inoue K, Yoshimura K. Skin stem cells. Methods Mol Biol 2013; 989:305-313.

38. Dai M, Wang P, Boyd AD, Kostov G, Athey B, Jones EG, Bunney WE, Myers RM, Speed TP, Akil H, Watson SJ, Meng F. Evolving gene/transcript definitions significantly alter the interpretation of GeneChip data. Nucleic Acids Res 2005; 33(20):e175.

39. Botchkareva NV, Kahn M, Ahluwalia G, Shander D. Survivin in the human hair follicle. The Journal of investigative dermatology 2007; 127(2):479-482.

40. Kleinpenning MM, Smits T, Frunt MH, van Erp PE, van de Kerkhof PC, Gerritsen RM. Clinical and histological effects of blue light on normal skin. Photodermatol Photoimmunol Photomed 2010; 26(1):16-21.

41. Mignon C, Uzunbajakava NE, Raafs B, Botchkareva NV, Moolenaar M, Tobin DJ. Photobiomodulation of distinct lineages of human dermal fibroblasts: a rational approach towards the selection of effective light parameters for skin rejuvenation and wound healing. 2016; SPIE 9695, Mechanisms of Photobiomodulation Therapy XI, 969508. SPIE Proceedings.

42. Inoue K, Aoi N, Sato T, Yamauchi Y, Suga H, Eto H, Kato H, Araki J, Yoshimura K. Differential expression of stem-cell-associated markers in human hair follicle

epithelial cells. Laboratory investigation; a journal of technical methods and pathology 2009; 89(8):844-856.

43. Ohyama M, Terunuma A, Tock CL, Radonovich MF, Pise-Masison CA, Hopping SB, Brady JN, Udey MC, Vogel JC. Characterization and isolation of stem cell-enriched human hair follicle bulge cells. The Journal of clinical investigation 2006; 116(1):249-260.

44. Kloepper JE, Tiede S, Brinckmann J, Reinhardt DP, Meyer W, Faessler R, Paus R. Immunophenotyping of the human bulge region: the quest to define useful in situ markers for human epithelial hair follicle stem cells and their niche. Exp Dermatol 2008; 17(7):592-609.

45. Purba TS, Haslam IS, Poblet E, Jimenez F, Gandarillas A, Izeta A, Paus R. Human epithelial hair follicle stem cells and their progeny: current state of knowledge, the widening gap in translational research and future challenges. Bioessays 2014; 36(5):513-525.

46. Karu TI. Cellular and Molecular Mechanisms of Photobiomodulation (Low-Power Laser Therapy). IEEE JOURNAL OF SELECTED TOPICS IN QUANTUM ELECTRONICS 2014; 20(2).

47. Wang Y, Huang YY, Wang Y, Lyu P, Hamblin MR. Photobiomodulation (blue and green light) encourages osteoblastic-differentiation of human adipose-derived stem cells: role of intracellular calcium and light-gated ion channels. Sci Rep 2016; 6:33719.

48. Hoang N, Schleicher E, Kacprzak S, Bouly JP, Picot M, Wu W, Berndt A, Wolf E, Bittl R, Ahmad M. Human and Drosophila cryptochromes are light activated by flavin photoreduction in living cells. PLoS biology 2008; 6(7):e160.

49. Anders JJ, Lanzafame RJ, Arany PR. Low-level light/laser therapy versus photobiomodulation therapy. Photomed Laser Surg 2015; 33(4):183-184.

50. Karu T. Mitochondrial Signaling in Mammalian Cells Activated by Red and Near-IR Radiation. Photochemistry and photobiology 2008; 84(5):1091-1099.

51. Karu TI, Pyatibrat LV, Afanasyeva NI. A novel mitochondrial signaling pathway activated by visible-to-near infrared radiation. Photochemistry and photobiology 2004; 80(2):366-372.

52. Passarella S, Karu T. Absorption of monochromatic and narrow band radiation in the visible and near IR by both mitochondrial and non-mitochondrial photoacceptors results in photobiomodulation. Journal of photochemistry and photobiology B, Biology 2014; 140:344-358.

53. Philpott MP, Sanders D, Westgate GE, Kealey T. Human hair growth in vitro: a model for the study of hair follicle biology. J Dermatol Sci 1994; 7 Suppl:S55-72.

54. Avci P, Gupta GK, Clark J, Wikonkal N, Hamblin MR. Low-level laser (light) therapy (LLLT) for treatment of hair loss. Lasers in surgery and medicine 2014; 46(2):144-151.

55. Leavitt M, Charles G, Heyman E, Michaels D. HairMax LaserComb laser phototherapy device in the treatment of male androgenetic alopecia: A randomized, double-blind, sham device-controlled, multicentre trial. Clin Drug Investig 2009; 29(5):283-292.

56. Vladimirov Iu A, Klebanov GI, Borisenko GG, Osipov AN. [Molecular and cellular mechanisms of the low intensity laser radiation effect]. Biofizika 2004; 49(2):339-350.

57. Khan I, Arany P. Biophysical Approaches for Oral Wound Healing: Emphasis on Photobiomodulation. Adv Wound Care (New Rochelle) 2015; 4(12):724-737.

58. Kim M, An J, Kim KS, Choi M, Humar M, Kwok SJ, Dai T, Yun SH. Optical lens-microneedle array for percutaneous light delivery. Biomed Opt Express 2016; 7(10):4220-4227.

59. Benitah SA, Valeron PF, van Aelst L, Marshall CJ, Lacal JC. Rho GTPases in human cancer: an unresolved link to upstream and downstream transcriptional regulation. Biochim Biophys Acta 2004; 1705(2):121-132.

60. Huang Z, Traugh JA, Bishop JM. Negative control of the Myc protein by the stress-responsive kinase Pak2. Mol Cell Biol 2004; 24(4):1582-1594.

61. Benitah SA, Frye M, Glogauer M, Watt FM. Stem cell depletion through epidermal deletion of Rac1. Science 2005; 309(5736):933-935.

62. McDowall M, Edwards NM, Jahoda CA, Hynd PI. The role of activins and follistatins in skin and hair follicle development and function. Cytokine Growth Factor Rev 2008; 19(5-6):415-426.

63. Miyagi M, Yokoyama H, Shiraishi H, Matsumoto M, Ishii H. Simultaneous quantification of retinol, retinal, and retinoic acid isomers by high-performance liquid chromatography with a simple gradiation. J Chromatogr B Biomed Sci Appl 2001; 757(2):365-368.

64. Becker A, Klapczynski A, Kuch N, Arpino F, Simon-Keller K, De La Torre C, Sticht C, van Abeelen FA, Oversluizen G, Gretz N. Gene expression profiling reveals aryl hydrocarbon receptor as a possible target for photobiomodulation when using blue light. Sci Rep 2016; 6:33847.

65. Masson-Meyers DS, Bumah VV, Enwemeka CS. Blue light does not impair wound healing in vitro. Journal of photochemistry and photobiology B, Biology 2016; 160:53-60.

66. Prabhu VR, Bola Sadashiva S.; Mahato, Krishna Kishore. Alterations in cell migration and cell viability of wounded human skin fibroblasts following visible red light exposure. Proceedings of the SPIE; 8932.

67. Pellicioli AC, Martins MD, Dillenburg CS, Marques MM, Squarize CH, Castilho RM. Laser phototherapy accelerates oral keratinocyte migration through the modulation of the mammalian target of rapamycin signaling pathway. J Biomed Opt 2014; 19(2):028002.

68. Song S, Zhang Y, Fong C-C, Tsang C-H, Yang Z, Yang M. cDNA Microarray Analysis of Gene Expression Profiles in Human Fibroblast Cells Irradiated with Red Light. Journal of Investigative Dermatology 2003; 120(5):849-857.

Figure Legends

Figure 1: Expression of Opsins in human hair follicle. (A) RT-PCR: only *OPN2* and *OPN3* were amplified from HFs cDNA, whilst Opsin1 short and middle wavelength (OPN1sw and *OPN1mw*), OPN4 and OPN5 amplicons were not detected. Human retina (R) or HaCaT cell line cDNA were used as positive controls. (**B)** RT-qPCR: relative expression of *OPN2* and *OPN3* were measured in anagen micro-dissected HFs from 6 patients of different gender and age. *OPN2* transcript levels are expressed at the higher level than *OPN3* in 5 out of 6 patients. Sex and age of each donor are below bar clusters (mean ±SD; n=2). Abbreviations: M – male; F – female

Figure 2: Localisation of OPN2 (Rhodopsin) in human skin. Immunofluorescence: **(A)** OPN2 (red) is expressed in the epidermis and dermal fibroblasts (arrows). **(B)** OPN2 (red) expression in the basal layer of epidermis, which is co-localised with CK14 (green, arrow-heads). **(C)** Expression of OPN2 (red) in anagen HFs along the ORS. **(D-E)** OPN2 (red) expression in the lower outer root sheath in terminal (**D**, arrows) and vellus (**E**, asterisk) HFs. **(F-G)** Co-expression of OPN2 (red) with CD200 (green), a marker of stem cells in human HFs. Scale bar 50 μm. Nuclear staining: DAPI (blue). Abbreviations: DP - dermal papilla; ORS - outer root sheath.

Figure 3: Localisation of OPN3 in human skin: **(A)** OPN3 (green) is expressed in the epidermis and in the dermal fibroblast (arrows); OPN3 (green) is expressed in the inner root sheath of terminal anagen HFs of female scalp (**B**) and vellus HF in male facial skin (**C**). **(D-E)** Double immunostaining of OPN3 (green) with either trichohyalin (AE15, red) or hair cortex cytokeratin (AE13, red): OPN3 is co-localized with AE15, but not with AE13. Scale bar 50 μm. Nuclear staining: DAPI (blue). Abbreviations: DP - dermal papilla; IRS - inner root sheath

Figure 4: mRNA expression of *OPN2* and *OPN3* is detected in the hair follicle stem cells. HFSC were sorted from total skin (n=3; 43-70-y-o). (**A**) Representative dot-plots showing 2 populations of HFSC: CD200+/CD49f+ cells and CD34+/CD200. (**B**) RT-qPCR: *OPN2* and *OPN3* expression was detected in both CD200+ and CD34+ enriched stem cell populations obtained from three donors. (mean ±SD; n=3). Abbreviation: F – female

Figure 5: Effects of OPN3 on the outer root sheath (ORS) cells *in vitro*. (**A**) RT-PCR: *OPN2* and *OPN3* transcripts were detected in the ORS keratinocytes *in vitro*. (**B**) No morphological changes were observed in the ORS cells after 48 h of OPN3 silencing (siOPN3). (**C**) RT-qPCR: dramatic decrease in *OPN3* expression (83%) in the ORS cells due to OPN3 siRNA transfection (mean ±SD; n=3). (**D**) Microarray validations by RT-qPCR: knock-down of OPN3 induced downregulation of *ULBP1, PAK 2, FSTL1, UBR5* and upregulation of *BLOC1S2, CAV2, SFXN1* expression (mean ±SD; n=3).

Figure 6: Effects of 3.2 J/cm^2 of blue light with 453 nm central wavelength on hair follicle growth *ex vivo*. (**A**) Representative microphotographs of anagen and catagen HFs at day 0 and day 7 of the experiment. (**B**) Effects of medium conditions (with insulin versus no insulin), donors and light treatment (blue and red light) on anagen to catagen transition expressed as mean survival time with 95% confidence intervals: insulin depletion caused premature catagen development as expected; donor effect was statistically significant (p=0.012), low levels of blue light increased mean survival time, improving anagen maintenance (pairwise comparison control vs blue light, significant at 10% level, p=0.066, mean ±SE); red light effect was not statistically significant (p=0.7). (**C**) Immunofluorescence: detection of proliferative Ki-67+ cells (green) in the hair matrix. Scale bar 50 µm. Nuclear staining: DAPI (blue); quantitative analysis revealed the statistically increased number of Ki-67+ cells in the HF treated with blue light (mean ±SD; p=0.04, Student's t-test); (**D**) Alamar assay: increase in metabolic activity in the ORS keratinocytes *in vitro* after 3.2 J/cm^2 of blue

light (n=3; mean ± SD, $p<0.05$, Student's t-test). (**E**) EdU assay: the number of proliferating ORS cells is significantly increased 8 hours after blue light irradiation (n=4; mean ± SD, $p=0.004$, Student's t-test). (**F**) Silencing of OPN3 in the ORS cells by siRNA significantly decreases proliferation rate compared to the control (scrambled) RNA and significantly represses proliferation induced by 3.2 J/cm^2 blue light ($p<0,0001$, two-way ANOVA test). Abbreviations: siSc - siRNA scrambled (negative RNA control); siOPN3 - siRNA against OPN3

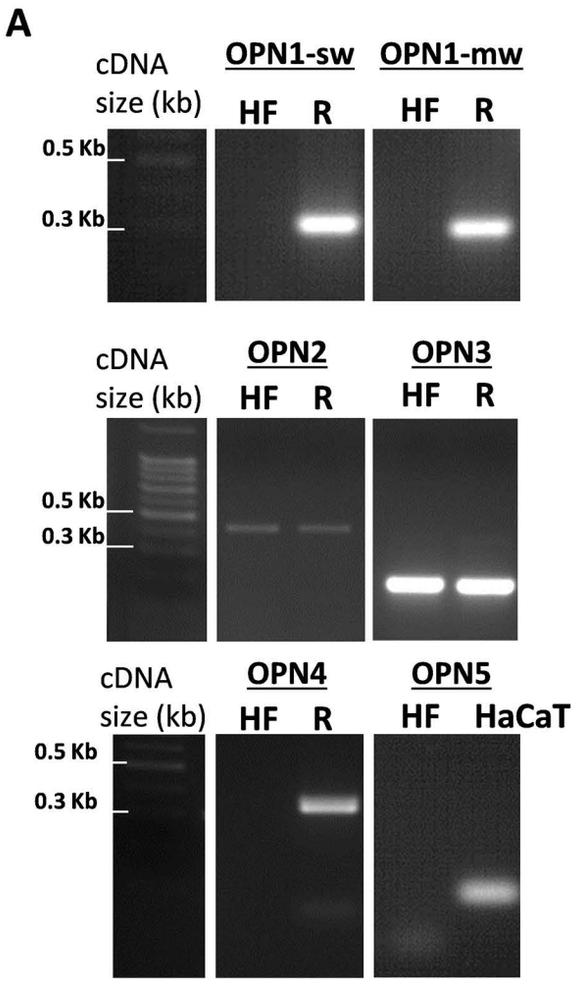

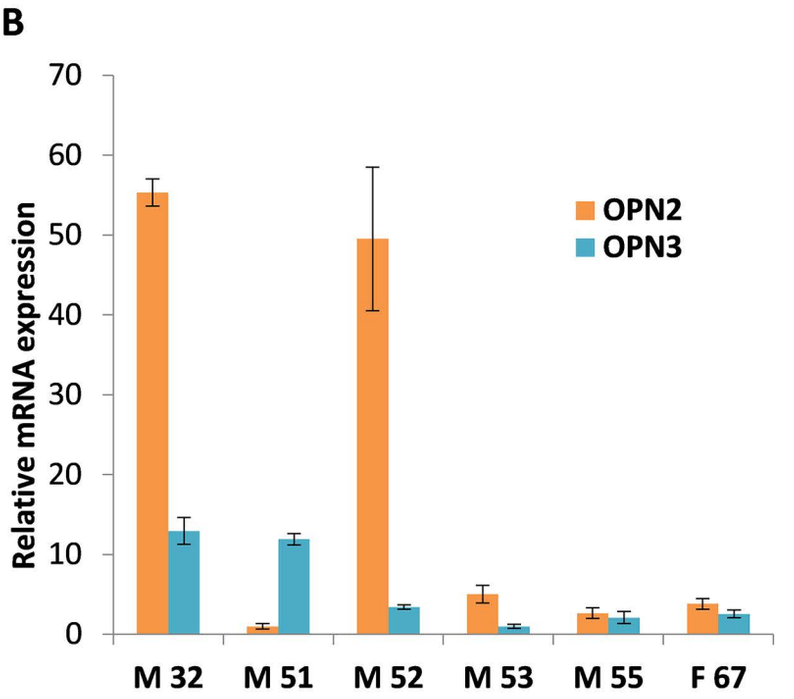

Figure 1, Buscone et al

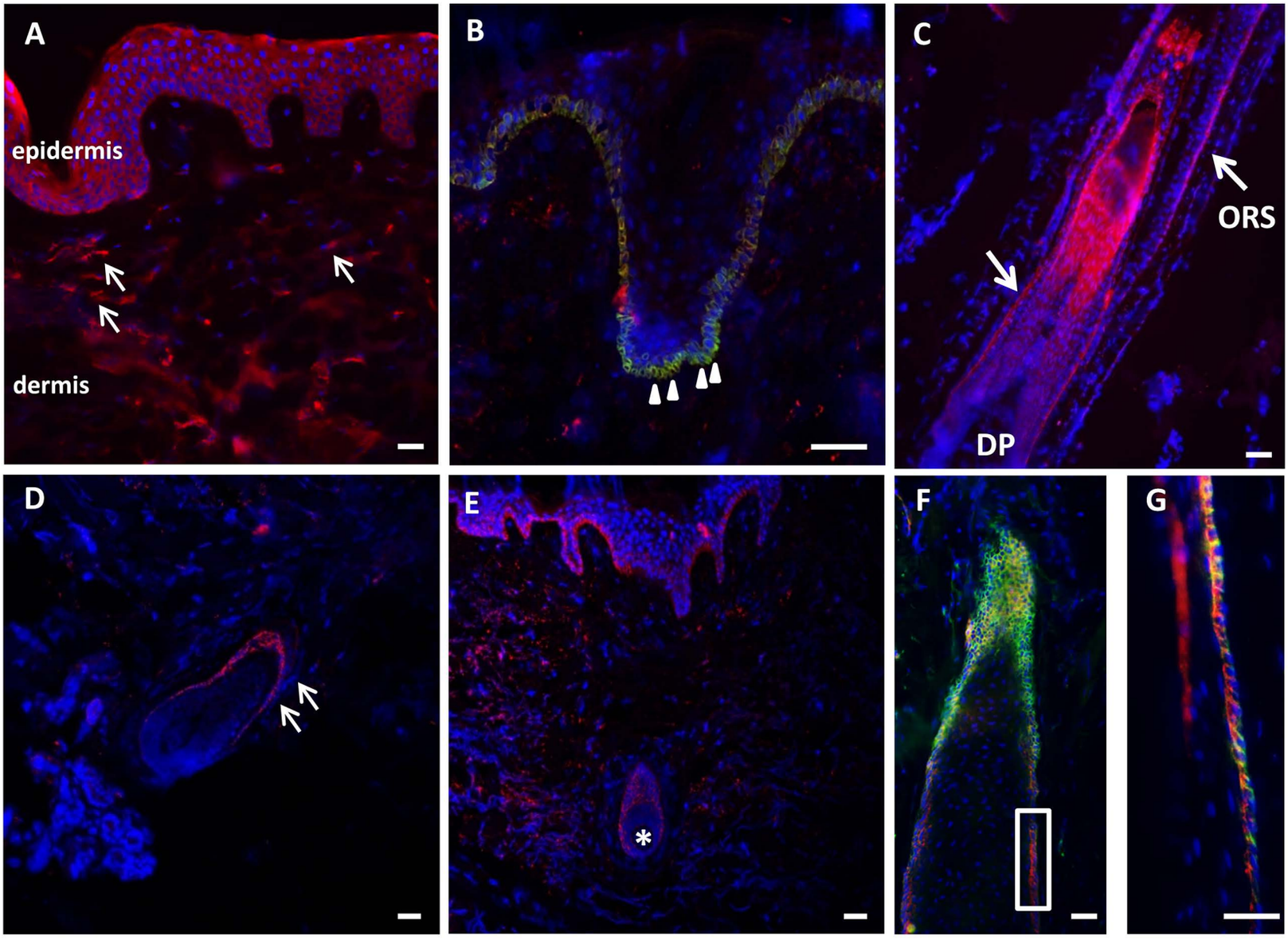

Figure 2, Buscone et al

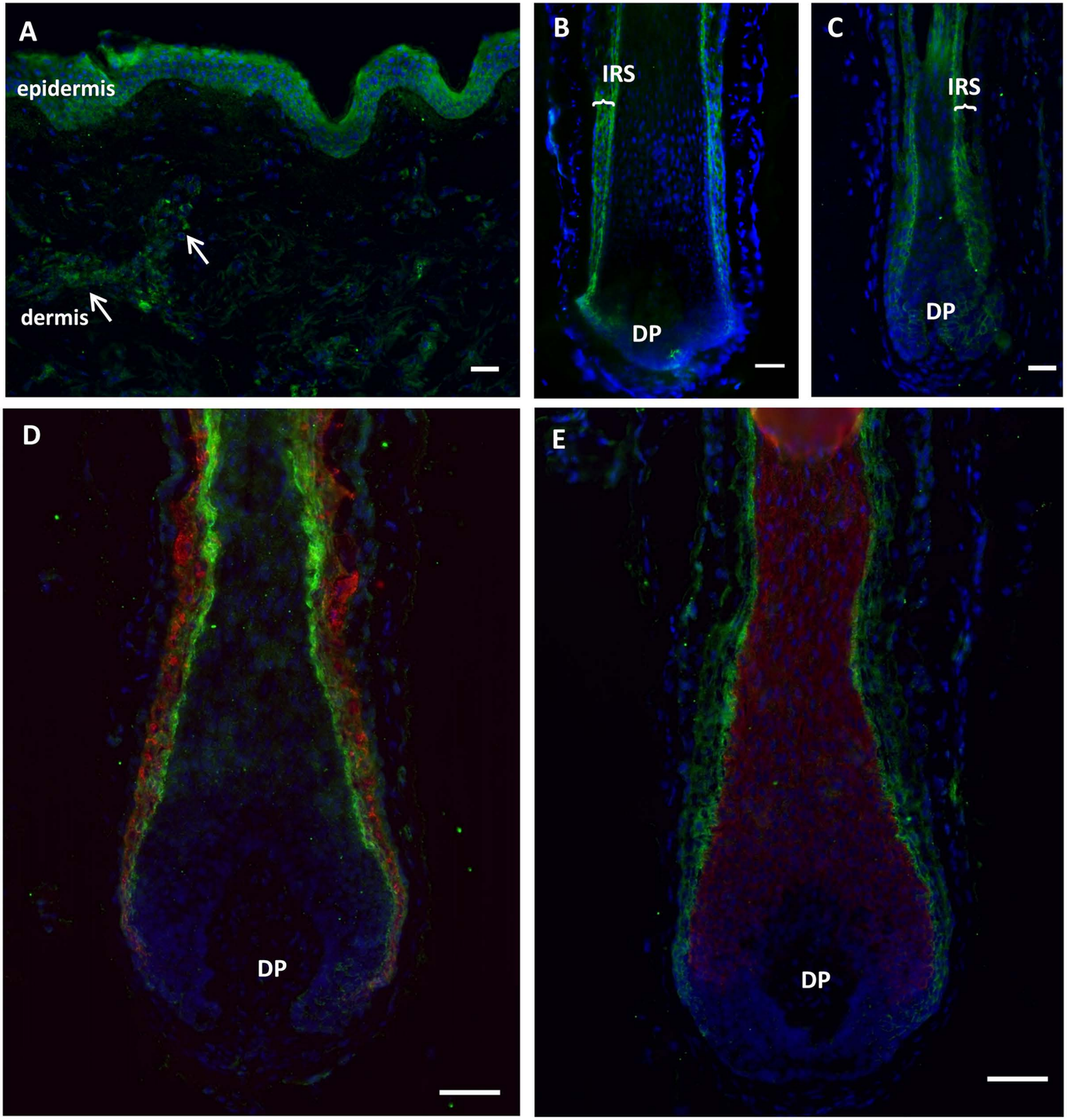

Figure 3, Buscone et al

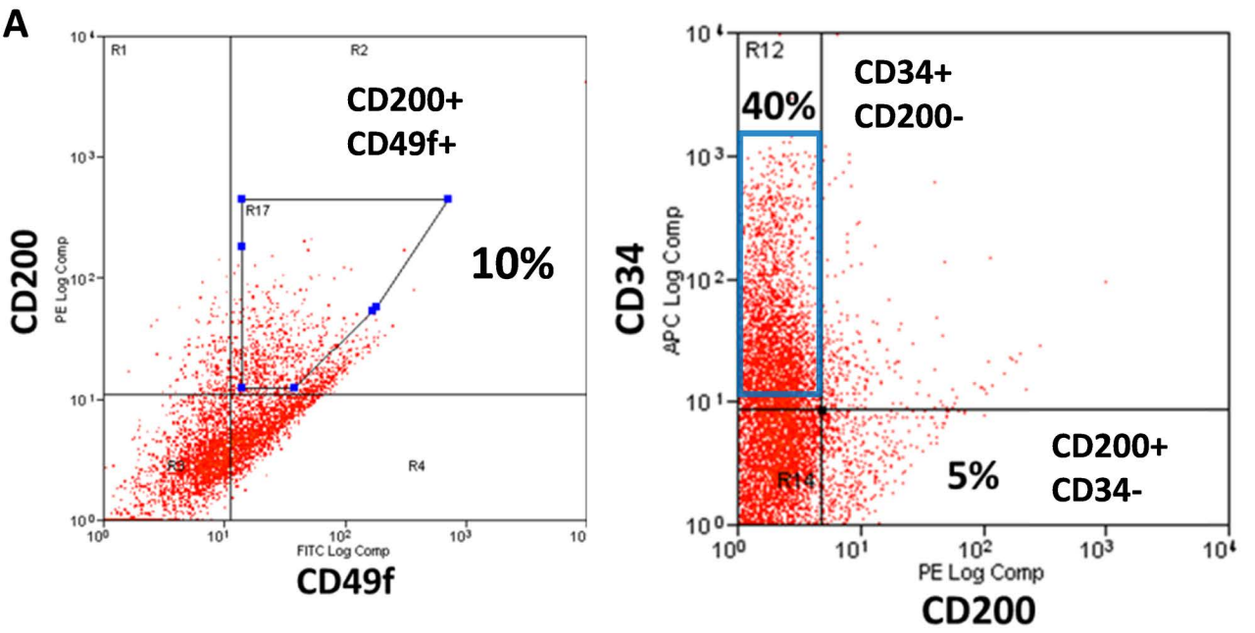

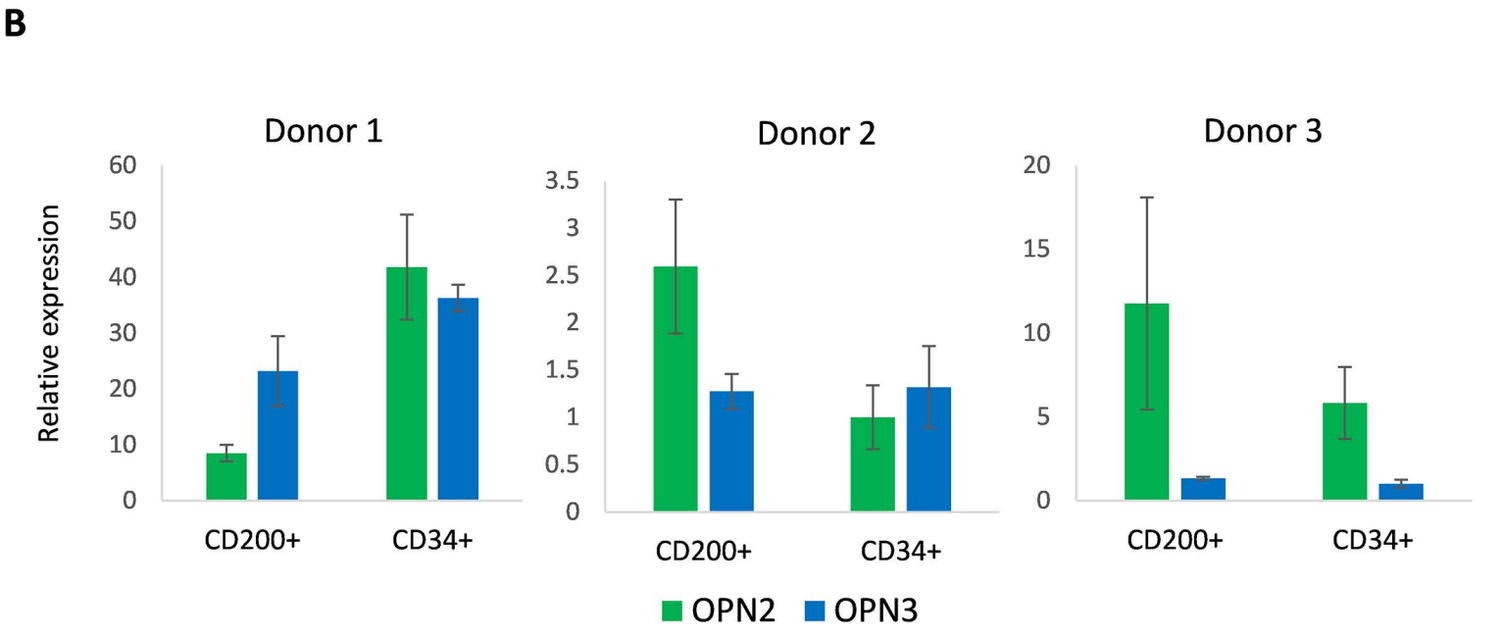

Figure 4, Buscone et al

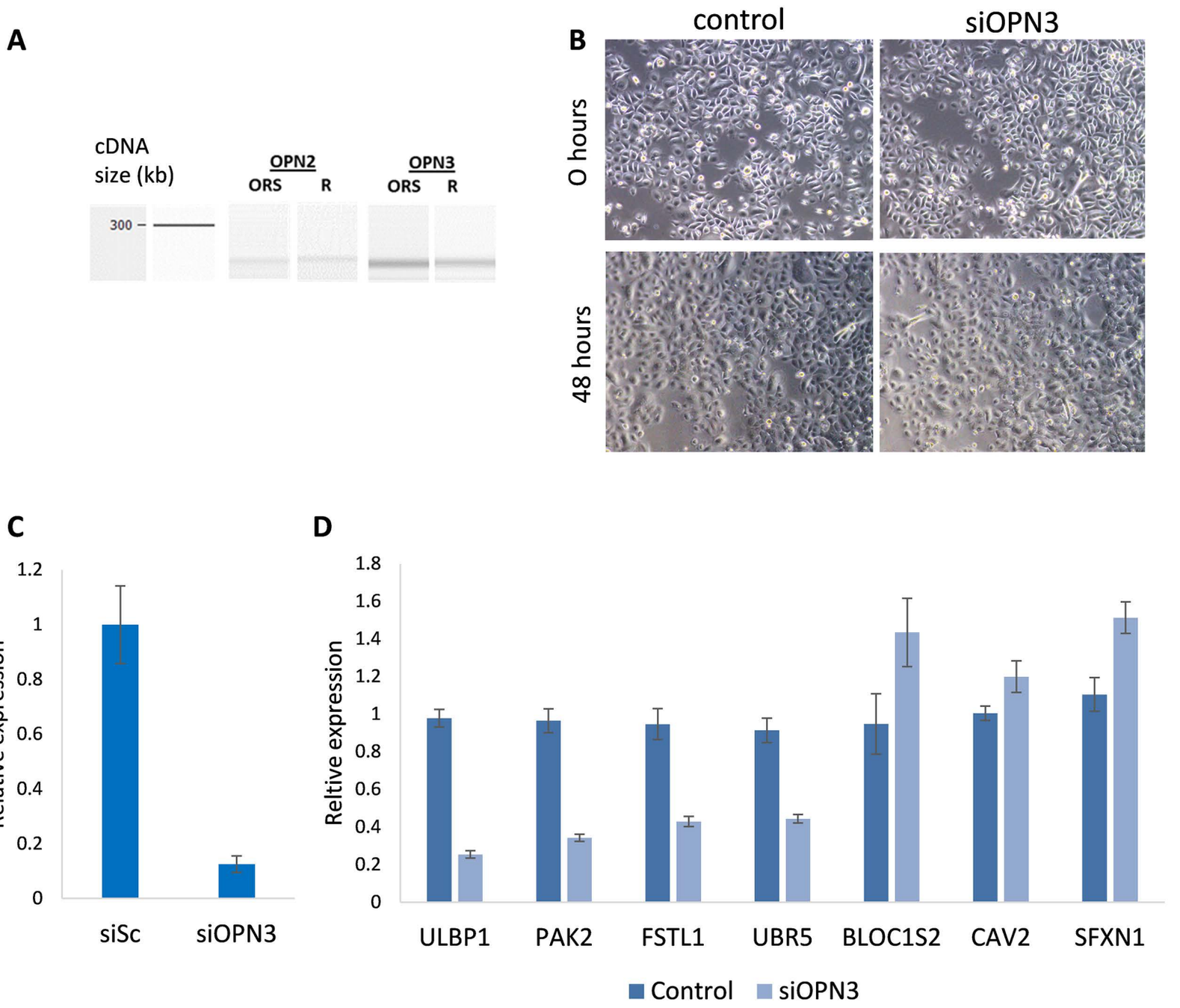

Figure 5, Buscone et al

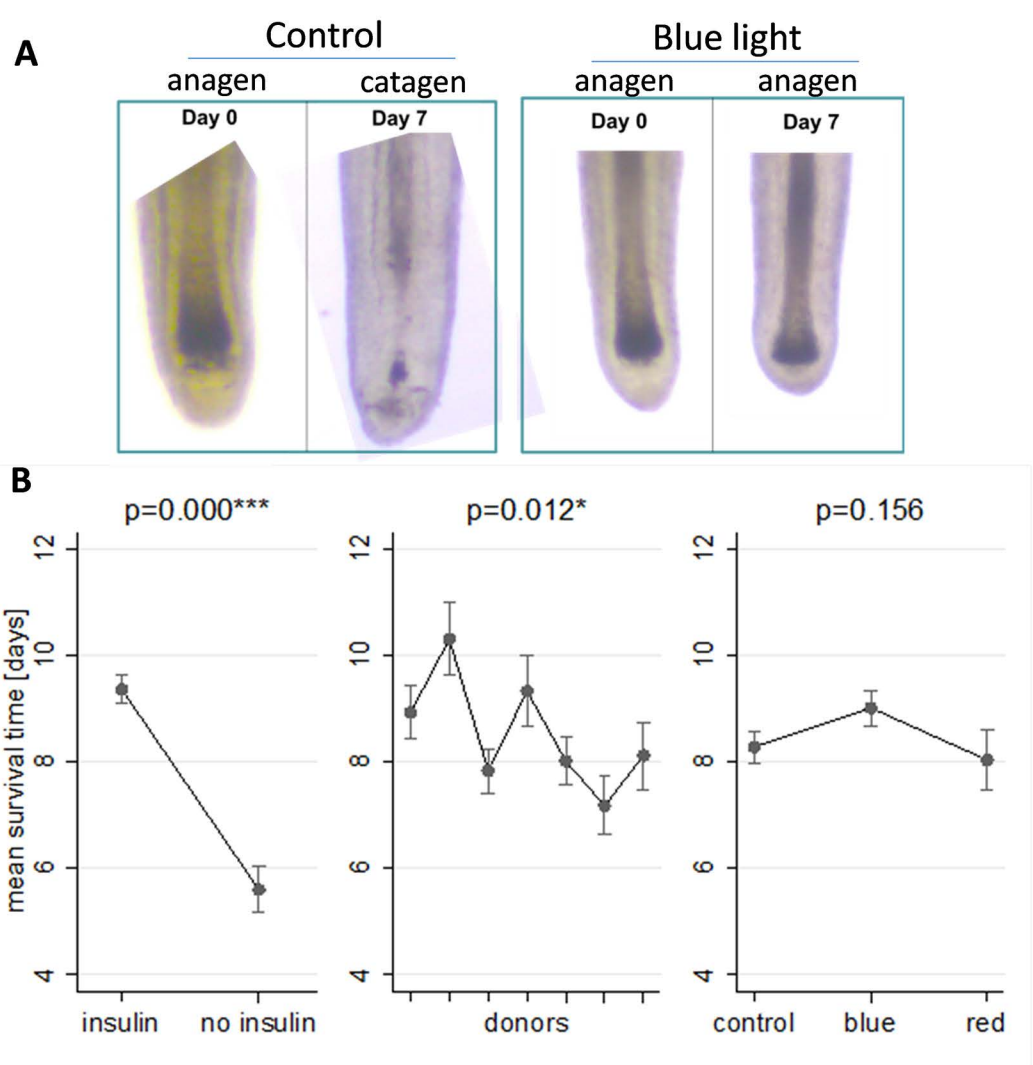

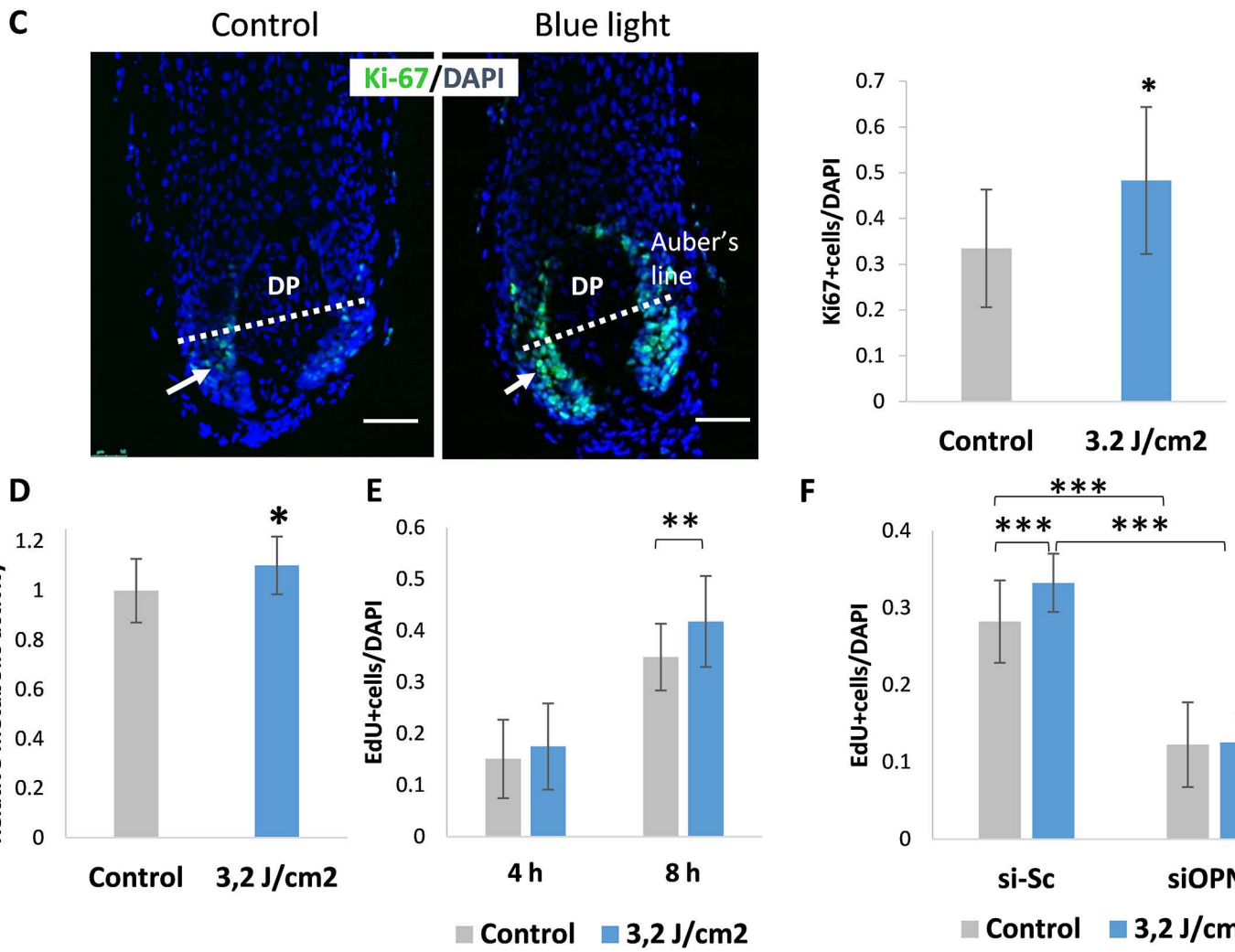

Figure 6, Buscone et al